Characterizing the primordial cosmic perturbations using MAP and Planck

Martin Bucher,* Kavilan Moodley,† and Neil Turok‡

DAMTP, Centre for Mathematical Sciences, University of Cambridge, Wilberforce Road, Cambridge CB3 0WA, United Kingdom

The most general homogeneous and isotropic statistical ensemble of linear scalar perturbations regular at early times in a universe with only photons, baryons, neutrinos, and a cold dark matter (CDM) component is described by a 5×5 symmetric matrix-valued generalization of the power spectrum. This description is complete if the perturbations are Gaussian, and even in the non-Gaussian case determines the expectation values of all observables quadratic in the small perturbations. The matrix valued power spectrum describes the auto and cross correlations of the adiabatic, baryon isocurvature, CDM isocurvature, neutrino density isocurvature, and neutrino velocity isocurvature modes. In this paper we examine the prospects for constraining or discovering isocurvature modes using forthcoming MAP and Planck measurements of the cosmic microwave background (CMB) anisotropy. We also consider the degradation in estimates of the cosmological parameters resulting from the inclusion of these modes. In the case of the MAP measurement of the temperature alone, the degradation is catastrophic. When isocurvature modes are admitted, uncertainties in the amplitudes of the mode auto- and cross correlations, and in the cosmological parameters, become of order one. With the inclusion of polarization (at an optimistic sensitivity) the situation improves for the cosmological parameters, but the isocurvature modes are still only weakly constrained. Measurements with Planck's estimated errors are far more constraining once polarization is included. If Planck operates as planned, the amplitudes of isocurvature modes will be constrained to less than 10% of the adiabatic mode, and simultaneously key cosmological parameters will be estimated to within a few percent or better.

I. INTRODUCTION

Because the physics by which cosmological perturbations imprint themselves on the cosmic microwave background (CMB) sky is very nearly linear, CMB observations offer a clean and comparatively direct probe of the nature of the primordial perturbations. The Cosmic Background Explorer (COBE) satellite established a normalization for the perturbation amplitude on large scales [1]. More recent CMB results [2–4] indicate a first Doppler peak with hints of further peaks that are beginning to constrain severely the space of allowed cosmological models. With the new forthcoming data from the Microwave Anisotropy Probe (MAP) satellite [5], launched in 2001, and from the Planck satellite [6], to be launched in 2007, this situation will greatly improve. It is hoped that one will be able to determine a host of cosmological parameters with great precision from the CMB data alone [7].

The assumption underlying this program is that the primordial fluctuations were adiabatic, that is, the relative abundances of different particle species were unperturbed from their thermal equilibrium values. This assumption has the great merit of simplicity, and is even justified in many specific models of the origin of the fluctuations. But given its central role in drawing inferences based on the CMB anisotropy, it seems worthwhile to attempt to verify the assumption of adiabaticity using the CMB data.

Cosmic inflation provides the best current explanation for

the origin of the perturbations, simultaneously explaining the large scale flatness and smoothness of the Universe [8,9]. In the simplest inflationary models the perturbations are indeed predicted to be Gaussian and adiabatic, with a nearly scale invariant power spectrum. But it is important to note that adiabaticity is not so much a generic consequence of inflation as the assumption that no additional information beyond the overall curvature perturbation on constant density slices survived the inflationary era. If fields exist that were perturbed during inflation so that their excitations survived into the postinflationary era before decaying in a nonadiabatic manner, then isocurvature perturbations generically would have been produced. Many inflationary models have been constructed in which this occurs. Given that no single compelling inflationary model exists and that most unified theories incorporating inflation invoke a great number of additional fields, it seems premature to associate the prediction of adiabaticity with inflation [10].

This situation motivates a more phenomenological approach to analyzing the new data that contemplates a wider range of possibilities for the nature of the primordial fluctuations and seeks to infer *from the data* what limits may be set on nonadiabatic perturbations. In a previous paper we examined the most general primordial perturbation possible in a cosmological model with no new physics—with only baryonic matter (and its associated electrons), photons, neutrinos, and a cold dark matter component, which is regular at early times [11]. *Primordial* here refers to the assumption that the perturbations were generated well before recombination, $z \approx 1100$, so that any singular (i.e., decaying) modes that may have been produced had ample opportunity to decay away before leaving an observable imprint on the CMB. In this work we found five regular modes: an adiabatic growing

---

*Email address: m.a.bucher@damtp.cam.ac.uk
†Email address: k.moodley@damtp.cam.ac.uk
‡Email address: n.g.turok@damtp.cam.ac.uk

mode, a baryon isocurvature mode, a CDM isocurvature mode, a neutrino density isocurvature mode, and a neutrino velocity isocurvature mode. The adiabatic growing mode assumes a common equation of state, spatially uniform everywhere in the universe. For the baryon isocurvature mode, the ratio of baryons to photons varies spatially [12–14], and similarly for the CDM isocurvature mode the ratio of CDM to photons varies spatially [15]. For the neutrino isocurvature modes, perturbations in the neutrino energy and momentum densities are balanced by opposing perturbations in the photon-radiation component, so that at early times the total stress-energy perturbation vanishes. At later times, however, the differences in how photons and neutrinos evolve lead to perturbations in the total stress-energy, which generate perturbations in the gravitational potentials, which in turn cause the baryons and CDM to cluster. Upon entering the horizon, the neutrinos simply free stream while the photons undergo strong Thomson scattering off free electrons, consequently behaving as a perfect fluid. The neutrino isocurvature modes, discussed in detail in Ref. [11], are implicit in the work of Rebhan and Schwarz [16] and of Challinor and Lasenby [17]; however, these authors do not investigate their implications. If Gaussian perturbations produced by a spatially homogeneous and isotropic random process are assumed, the most general perturbation of the five regular modes is completely described by the 5×5, symmetric correlation matrix

$$P_{ij}(k) = \langle A_i(\mathbf{k})A_j(-\mathbf{k}) \rangle \qquad (1)$$

where $(i,j = 1, \ldots, 5)$ labels the modes and $A_i(\mathbf{k})$ indicates the amplitude of the ith mode with wave vector $\mathbf{k}$. This generalizes the usual scalar power spectrum. In the case of non-Gaussian perturbations, the above matrix suffices to determine the expectation values of all perturbations quadratic in the small perturbation (this includes the CMB power spectrum) as long as the linearized theory is valid.

The possibility of ascribing cosmological perturbations entirely to isocurvature modes, either to the baryon isocurvature mode or to the CDM isocurvature mode, has previously been considered, and these possibilities were found inconsistent with the existing observational data [18–26]. However, apart from the work of Enqvist and Kurki-Suonio [27] and of Pierpaoli, García-Bellido, and Borgani [28], little effort has been devoted to the problem of detecting or constraining admixtures of isocurvature modes observationally. Moreover, when one admits the possibility of more than one mode being excited, the possibility arises of correlations of several modes. These are characterized by the off-diagonal elements of $P_{ij}(k)$. Linde and Mukhanov [29], Langlois [30], and Langlois and Riazuelo [31], drawing on the work of Polarski and Starobinskii [32] on double inflation, investigated an inflationary model with two scalar fields exciting both the adiabatic and baryon isocurvature modes in varying proportions and with various degrees of correlation between these modes. In an inflationary model with five or more scalar fields (or a single field with the same number of real components), it is generically possible to realize the most general $P_{ij}(k)$ of the form discussed above.

The reader might suspect that we are in effect opening a Pandora's box of possibilities for the primordial perturbations, which experiment will never be able to close. Certainly if one allows $P_{ij}(k)$ to be an arbitrary function of k, there is such huge freedom that one might be able to fit almost any conceivable observational results. However, the situation is not so bad if one restricts attention to power spectra which are smooth over the observed range of wave numbers. In fact we shall assume that all the isocurvature power spectra concerned are scale invariant in the sense defined below, so that they contribute across a broad range of scales accessible to the CMB. This assumption could easily be extended to more general power law spectra.

Another way of viewing our results may make this approach more palatable. That is, we should think of the observed Universe as the outcome of a huge high energy experiment. By studying what emerged from this event, we hope to gain information about high energy processes in the very early universe which we cannot directly view. Therefore, the primordial plasma is a giant detector, within which the interesting event occurred. Clearly, from this point of view it is worthwhile to understand all possible linear response modes (i.e., all "channels") and to study these to determine whether they were excited in the primordial universe. The question posed in this paper is whether one can check the extent to which the nonadiabatic channels in the CMB were actually excited in the early Universe, at least over the observationally relevant range of length scales.

The outline of the paper is as follows. Section II discusses the statistical techniques employed to interpret CMB measurements and reviews the properties of the five regular perturbation modes allowed. Section III presents numerical results in the form of eigenvectors and eigenvalues of the "Fisher matrix," corresponding to the MAP and Planck measurements. The tables provided allow one to calculate the uncertainty in any cosmological parameter or function thereof, as well as in the amplitudes of the primordial perturbation modes. Section IV discusses the significance of the results and our main conclusion, which is that a high precision measurement of the cosmic polarization anisotropy will be essential to measure cosmological parameters accurately while simultaneously establishing the character of the primordial perturbations.

We mention three limitations of our analysis. Our main goal is to explore the effect of relaxing the assumption of adiabaticity. Therefore we ignore tensor modes, which would only complicate the discussion. But many inflationary models do predict tensor modes and it is important to include them in any complete analysis. The second caveat is that we consider here only very subdominant isocurvature perturbations: our analysis is perturbative around a standard ΛCDM model. Finally, as mentioned above, we do not vary the spectral indices (or the shape of the spectra) for the isocurvature modes. We consider only "scale invariant" isocurvature perturbations as defined below. In inflationary models, isocurvature perturbations (like adiabatic ones) would in general have adjustable power spectra and again this fact would complicate the discussion.

II. THE GENERAL PRIMORDIAL COSMIC PERTURBATION

Statistical analysis of observational data, be it based on "classical" or "frequentist" statistics or on Bayesian statistics, ultimately reduces to considering relative likelihoods of competing theoretical descriptions given the observed data. Because the observational data is not yet available, we must assume a particular underlying theoretical model for computing expectations for relative likelihoods. We assume a statistical model with independent Gaussian distributions for the individual moments of the CMB multipole expansion with variance

$$\langle |a_{lm}|^2 \rangle = c_l + \sigma_{n,l}^2, \tag{2}$$

where c_l is the variance of the underlying cosmological signal and $\sigma_{n,l}^2$ is the variance resulting from detector noise. It follows that the expectation value of the logarithm of the relative likelihood of model B relative to model A under the assumption that the data were produced according to the distribution from model A is given by the formula

$$\left\langle \log\left[\frac{p_B}{p_A}\right] \right\rangle_A = \left\langle \log\left[\frac{p(\{a_{lm}\}|B)}{p(\{a_{lm}\}|A)}\right] \right\rangle_A$$

$$= \frac{f_{sky}}{2} \sum_{l=2}^{l_{max}} (2l+1) \left\{ 1 - \frac{c_{l,A} + \sigma_{n,l}^2}{c_{l,B} + \sigma_{n,l}^2} \right.$$

$$\left. + \log\left[\frac{c_{l,A} + \sigma_{n,l}^2}{c_{l,B} + \sigma_{n,l}^2}\right] \right\}, \tag{3}$$

where $\{a_{lm}\}$ is the observed data, $c_{l,A}$ and $c_{l,B}$ are the variances of the cosmological signal predicted by models A and B, respectively, and $\sigma_{n,l}^2$ is the Gaussian detector noise for each multipole of order l. The f_{sky} indicates the fraction of the sky remaining after the galaxy cut.

We consider cosmological models where c_l depends on a number of continuous parameters $\alpha_1, \ldots, \alpha_N$. With relatively little detector noise and with changes in the parameters affecting a large number of multipoles, in the region of interest where the likelihood relative to the reference model is comparable, the following quadratic approximation is justified

$$\left\langle \log\left[\frac{p(\alpha_1, \ldots, \alpha_N)}{p(\alpha_1^{(0)}, \ldots, \alpha_N^{(0)})}\right] \right\rangle_{(0)}$$

$$= -\frac{f_{sky}}{2} \sum_{i,j=1}^{N} \sum_{l=2}^{l_{max}} (2l+1) \times \frac{1}{(c_{l,A} + \sigma_{n,l}^2)^2} \frac{\partial c_l}{\partial \alpha_i} \frac{\partial c_l}{\partial \alpha_j}$$

$$\times \frac{(\alpha_i - \alpha_i^{(0)})(\alpha_j - \alpha_j^{(0)})}{2}. \tag{4}$$

We write the right-hand side as $-\frac{1}{2}F_{ij}(\alpha_i - \alpha_i^{(0)})(\alpha_j - \alpha_j^{(0)})$. In the case where the variations in the logarithm are described by a quadratic form, the matrix F_{ij} is equivalent to the Fisher matrix, and in the sequel we shall refer to it in this way even though the terminology is not completely accurate.

The quadratic approximation may break down when considering variations primarily affecting very low-l moments, where a Gaussian approximation to a χ^2-distribution of low order is inaccurate even near where it is peaked.

When polarization is included, Eq. (2) is modified to become

$$M_l = \begin{pmatrix} |\langle a_{lm} \, a_{lm} \rangle| & |\langle a_{lm} \, b_{lm} \rangle| \\ |\langle b_{lm} \, a_{lm} \rangle| & |\langle b_{lm} \, b_{lm} \rangle| \end{pmatrix}$$

$$= \begin{pmatrix} c_{l,T} + \sigma_{nl,T}^2 & c_{l,C} \\ c_{l,C} & c_{l,P} + \sigma_{nl,P}^2 \end{pmatrix}, \tag{5}$$

and Eq. (3) is modified to

$$\left\langle \log\left[\frac{p_B}{p_A}\right] \right\rangle_A = \left\langle \log\left[\frac{p(\{a_{lm}\}, \{b_{lm}\}|B)}{p(\{a_{lm}\}, \{b_{lm}\}|A)}\right] \right\rangle_A$$

$$= \frac{f_{sky}}{2} \sum_{l=2}^{l_{max}} (2l+1)[\mathrm{tr}\{I - M_{lA}M_{lB}^{-1}\}$$

$$+ \ln\{\det(M_{lA}M_{lB}^{-1})\}]. \tag{6}$$

The second derivative of the above may be expressed as

$$\delta^2 \left\langle \log\left[\frac{p_B}{p_A}\right] \right\rangle_A = f_{sky} \sum_{l=2}^{l_{max}} (2l+1)$$

$$\times \left[\mathrm{tr}\{(\delta M_l)M_{ref,l}^{-1}(\delta M_l)M_{ref,l}^{-1}\} \right.$$

$$+ \det\{(\delta M_l)M_{ref,l}^{-1}\}$$

$$\left. - \frac{1}{2}\mathrm{tr}^2\{(\delta M_l)M_{ref,l}^{-1}\} \right]. \tag{7}$$

Most studies of parameter estimation using future CMB data assume adiabatic perturbations from inflation allowing a set of model parameters, such as H_0, Ω_b, Ω_Λ, for example, to be varied. A fiducial, or reference, model is assumed, and the behavior of the relative likelihood in the neighborhood of this reference model is explored.

We extend this approach by including parameters for the strengths of the isocurvature modes and of their cross correlations, both with respect to one another as well as to the adiabatic mode. In this case the parametric model becomes the following:

$$c_l(\boldsymbol{\beta}, \boldsymbol{\gamma}, \boldsymbol{\delta}, \boldsymbol{\xi}) = c_l^{adia}(\beta_1, \ldots, \beta_N)$$

$$+ \sum_{A=1}^{4} \gamma_A \, c_l^A(\beta_1, \ldots, \beta_N)$$

$$+ \sum_{A=1}^{4} \delta_A \, c_l^{A-adia}(\beta_1, \ldots, \beta_N)$$

$$+ \sum_{\substack{A,B=1 \\ A \neq B}}^{4} \xi_{AB} \, c_l^{A-B,cross}(\beta_1, \ldots, \beta_N), \tag{8}$$

where the indices A, B label the four nonsingular isocurvature modes. Here the vector $\boldsymbol{\beta}$ represents the usual cosmological parameters. The vector $\boldsymbol{\gamma}$ indicates the autocorrelations of the isocurvature modes. The vector $\boldsymbol{\delta}$ indicates the cross correlation of the isocurvature modes with the adiabatic mode, and the symmetric off-diagonal elements ξ_{AB} indicate the cross correlations of the isocurvature modes with each other. The components c_l^A are computed with a modified version of CMBFAST [33] with the isocurvature mode excited. The cross correlations are computed by running CMBFAST, first with two modes excited and then subtracting the results with each mode individually excited, using the relation $Q(A,B) = \frac{1}{2}[Q(A+B,A+B) - Q(A,A) - Q(B,B)]$ valid for any quadratic form Q. From the viewpoint of the statistical analysis described above, all components of the combined vector $\boldsymbol{\alpha} = (\boldsymbol{\beta}, \boldsymbol{\gamma}, \boldsymbol{\delta}, \boldsymbol{\xi})$ stand on equal footing. The three components $\boldsymbol{\gamma}, \boldsymbol{\delta}, \boldsymbol{\xi}$ are related to the correlation matrix M given in Ref. [11] according to

$$M = \begin{pmatrix} 1 & \delta_1 & \delta_2 & \delta_3 & \delta_4 \\ \delta_1 & \gamma_1 & \xi_{1,2} & \xi_{1,3} & \xi_{1,4} \\ \delta_2 & \xi_{2,1} & \gamma_2 & \xi_{2,3} & \xi_{2,4} \\ \delta_3 & \xi_{3,1} & \xi_{3,2} & \gamma_3 & \xi_{3,4} \\ \delta_4 & \xi_{4,1} & \xi_{4,2} & \xi_{4,3} & \gamma_4 \end{pmatrix}. \qquad (9)$$

Some free parameters of our model cannot be treated in the same way as the ones above when the fiducial model is purely adiabatic with no isocurvature component excited. These include the spectral indices for the isocurvature modes. The difficulty arises because near the fiducial model the dependence on these spectral indices vanishes. In this paper we simply fix the spectral indices to correspond to "scale invariant" isocurvature perturbations. For simplicity we also choose the cross-correlation power spectra to have a k dependence corresponding to the geometric mean of the autocorrelation power spectra for the two variables. This assumption is straightforward to generalize.

Figure 1 shows the C_l temperature power spectra for the modes considered. We choose as our fiducial cosmological model $h = 0.65$, $\Omega_b = 0.06$, $\Omega_\Lambda = 0.69$, $\Omega_{cdm} = 0.25$, $n_S = 1$, and a small amount of reionization with an optical depth to the last scattering surface of $\tau = 0.1$. In Fig. 1, $l(l+1)C_l/2\pi$ from adiabatic scale-invariant perturbations is plotted as well as the same quantity for baryon isocurvature, neutrino isocurvature density, and neutrino isocurvature velocity modes. For the baryon isocurvature mode a scale free spectrum for $\delta(\rho_B/\rho_\gamma)$ is assumed (i.e., the variance at early times is a logarithmically divergent integral over wave number). For neutrino isocurvature density perturbations a scale free spectrum is assumed for $\delta(\rho_\nu/\rho_\gamma)$ and for neutrino isocurvature velocity perturbations a scale free spectrum is assumed for the bulk neutrino velocity v_ν. The CMB spectrum for the CDM isocurvature mode agrees with that obtained for the baryon isocurvature mode to a fraction of a percent. Therefore we do not consider the CDM isocurvature case separately, neither here nor in our numerical analysis. The lower panels of Fig. 1 show the $l(l+1)C_l/2\pi$ produced from the cross correlations of the allowed modes.
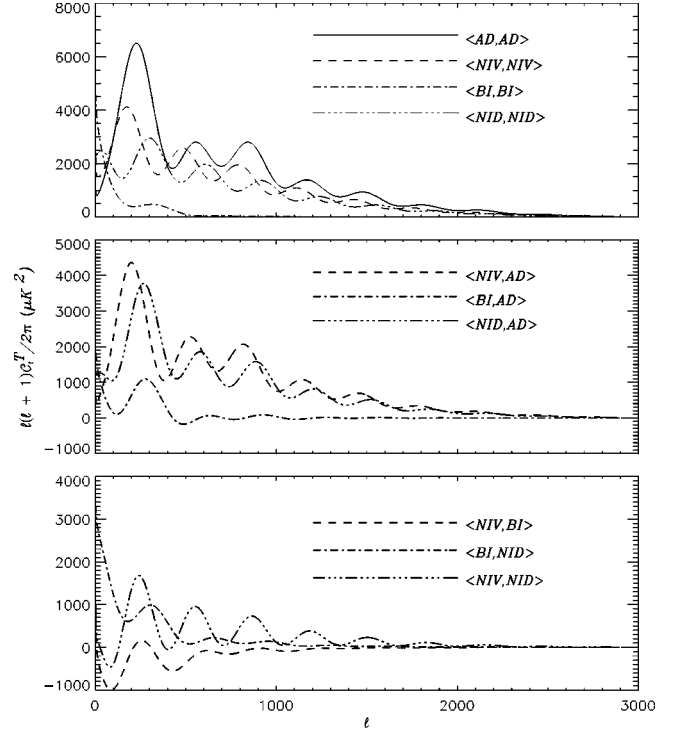

FIG. 1. CMB anisotropy temperature power spectra $l(l+1)C_l/2\pi$ are plotted versus l. The upper panel shows the adiabatic and isocurvature autocorrelation spectra, while the lower two panels illustrate the cross-correlation spectra of the various modes.

III. NUMERICAL RESULTS

We now proceed to our numerical results. Both the MAP and Planck experiments are considered, for which we use $l_{max} = 3000$. Following [34], we assume $f_{sky} \approx 0.8$ for the fractional sky coverage after the galaxy cut and ignore foreground contamination. Under these assumptions, it follows that

$$\frac{1}{\sigma_{n,l}^2} = \sum_c \frac{B_{l,c}^2}{\sigma_c^2 \theta_{\text{FWHM},c}^2} \qquad (10)$$

where c indicates the sum over channels, $B_{l,c}^2 = \exp[-(0.425\,\theta_{\text{FWHM},c}l)^2]$ is the window function assuming a Gaussian beam, with $\theta_{\text{FWHM},c}$ the full width at half maximum of the cth channel, and $\sigma_c^2 \theta_{\text{FWHM},c}^2$ is the mean square noise per multipole. The assumption of no correlations between pixels makes this quantity independent of l. For MAP we assume three channels (40, 60, and 90 GHz) with $\theta_{\text{FWHM},c} = 0.47°$, $0.35°$, and $0.21°$, and $\sigma_c = 22.3$, 30, and 50 μK, respectively, as anticipated after two years of data.[1] For Planck, we use the three lowest frequency channels (100, 143, and 217 GHz) of the high frequency instrument (HFI) with $\theta_{\text{FWHM},c} = 0.18°$, $0.13°$, and $0.092°$ and $\sigma_c = 4.5$, 5.5,

---

[1]$\sigma = 27$, 35, and 35 μK are the corresponding temperature errors for a $0.3°$ square pixel given in the Wang, Spergel, and Strauss paper [34]. The sensitivity of the 40 GHz channel has subsequently been downgraded to 35 μK, which is the value we assume here.

and 11.8 μK, respectively, as expected after 12 months of data (which would correspond to 2.7, 2.4, and 3.6 μK on a 0.3° square pixel).

We also indicate below the result of including polarization. For the two higher frequencies of the three Planck channels, for which polarization information will be available, we use the latest available sensitivities $\sigma_c^P = 10.18$ and 24.42 μK, respectively. For the MAP experiment, for which all three channels include polarization information, we assume that $\sigma_{nP}^2 = 2\sigma_{nT}^2$. Systematics and foreground effects not included here may introduce additional uncertainties into the cosmic polarization measurement. Nevertheless, we include calculations making the most optimistic assumption for comparative purposes and to emphasize what could be learned from an accurate polarization measurement.

We do not indicate an uncertainty in normalization because a natural way to compare relative normalizations between spectra of different shapes is lacking. Other authors indicate the uncertainty in the predicted expectation value for the quadrupole. This, however, is a not a very useful quantity given the large uncertainty from cosmic variance in the quadrupole. Instead we marginalize over the normalization. In the quadratic approximation this procedure is equivalent to using the best fit normalization for the given values of the parameters and amounts to replacing the Fisher matrix with the reduced Fisher matrix

$$\hat{F}_{ij} = F_{ij} - \frac{F_{i0}F_{j0}}{F_{00}}, \tag{11}$$

where the index 0 labels the parameter describing the overall normalization of the power spectrum.

We have computed the eigenvalues and eigenvectors (i.e., the spectral decomposition) of the reduced Fisher matrix $\hat{F}_{ij}$. These fully specify the likelihood function in the Gaussian approximation about the fiducial model, and in the same approximation fully determine the uncertainties in any cosmological parameters or perturbation amplitudes. Complete tables are made available on the following web page: http://www.damtp.cam.ac.uk/user/mab43/isocurvature/.

Evaluating the Fisher matrix above requires calculating the derivatives of the C_l spectrum with respect to the various parameters. The variations with respect to the mode amplitudes are exact while a judicious choice of step size allows one to determine accurately, using centered finite differences, the Ω_Λ, n_s, and τ derivatives. However, the CMB spectrum depends only indirectly on the parameters h and Ω_b, which makes these derivatives more susceptible to the numerical noise present in CMBFAST. They can be accurately determined by transforming from the derivatives calculated with respect to the physical parameters $\omega_m = (\Omega_{cdm} + \Omega_b)h^2$ and $\omega_b = \Omega_b h^2$, using the equations below:

$$\frac{1}{h}\frac{\partial}{\partial h} = \frac{2}{\omega_m}\frac{\partial}{\partial \omega_m} + \frac{2}{\omega_b}\frac{\partial}{\partial \omega_b}, \qquad \frac{1}{\Omega_b}\frac{\partial}{\partial \Omega_b} = \frac{1}{\omega_b}\frac{\partial}{\partial \omega_b}. \tag{12}$$

To avoid exposing the derivative with respect to Ω_k to the noisier "open" version of CMBFAST, we consider only variations in open models where the angular diameter distance is held fixed. This requires evaluating the derivative of the curvature indirectly through the use of the formula

$$\left(\frac{\partial}{\partial \Omega_k}\right)_{\Omega_\Lambda} = \left(\frac{\partial}{\partial \Omega_k}\right)_{d_A} + \frac{\left(\dfrac{\partial d_A}{\partial \Omega_k}\right)_{\Omega_\Lambda}}{\left(\dfrac{\partial d_A}{\partial \Omega_\Lambda}\right)_{\Omega_k}}\left(\frac{\partial}{\partial \Omega_\Lambda}\right)_{\Omega_k}, \tag{13}$$

where

$$d_A = \frac{1}{\sqrt{\Omega_k H_0^2}}\sinh\left[\sqrt{\Omega_k}\int_0^{z_{rec}}\frac{dz}{\sqrt{E(z)}}\right],$$

$$E(z) = \Omega_\Lambda + \Omega_k(1+z)^2 + (\Omega_{cdm} + \Omega_b)(1+z)^3 + \Omega_r(1+z)^4, \tag{14}$$

with Ω_r specifying the density of radiation today and z_{rec} the redshift of recombination. More details of these techniques can be found in [35].

We now present the main results of the above calculations. We consider a fiducial spatially flat cosmological model with $h = 0.65$, $\Omega_b = 0.06$, $\Omega_\Lambda = 0.69$, $\Omega_{cdm} = 0.25$, with scalar spectral index $n_S = 1$, and a small amount of reionization with an optical depth to the last scattering surface of $\tau = 0.1$. Variations in the parameters H_0, Ω_Λ, Ω_b, n_S, τ, and Ω_k are considered. Except for the last two of these parameters, all variations are considered fractionally. The density of cold dark matter Ω_{cdm} is defined implicitly as $\Omega_{cdm} = (1 - \Omega_\Lambda - \Omega_k - \Omega_b)$. The isocurvature modes are normalized so that their mean square power contribution to the CMB temperature anisotropy summed from $l=2$ to $l=3000$ is equivalent to that of the adiabatic mode. For one additional mode, two new parameters arise in addition to those described in the previous section: the isocurvature autocorrelation $\langle II \rangle$ and the cross correlation with the adiabatic mode $\langle AI \rangle$. The positive definiteness of the matrix valued power spectrum requires that $|\langle AI \rangle| \leq \sqrt{\langle II \rangle}$.

Table I shows the 1-σ percentage uncertainties for the cosmological parameters and isocurvature autocorrelation amplitudes, derived for the proposed MAP and Planck experiments. The top four lines show the uncertainties for the MAP temperature measurement, the combined MAP polarization-temperature measurement, the Planck temperature measurement, and the combined Planck polarization-temperature measurement, respectively, under the assumption that no isocurvature modes are present. Going down the

TABLE I. Percentage errors in cosmological parameters and mode admixture. Each block of four rows represents a varying number of isocurvature modes allowed, from none (top) to all three (bottom). Within each block, both MAP and Planck, with temperature only and with temperature and polarization, are considered.

	$\delta h/h$	$\delta\Omega_b/\Omega_b$	$\delta\Omega_k$	$\delta\Omega_\Lambda/\Omega_\Lambda$	$\delta n_s/n_s$	τ_{reion}	⟨NIV,NIV⟩	⟨BI,BI⟩	⟨NID,NID⟩	⟨NIV,AD⟩	⟨BI,AD⟩	⟨NID,AD⟩	⟨NIV,BI⟩	⟨NIV,NID⟩	⟨BI,NID⟩
MAP-T	12.38	27.78	9.80	12.95	7.03	37.46									
MAP-TP	7.61	13.70	2.79	5.12	1.65	2.00									
PL-T	11.38	22.72	5.91	2.28	0.54	9.98									
PL-TP	3.81	7.54	1.91	1.27	0.35	0.47									
MAP-T	12.51	28.34	9.90	13.70	8.08	39.38	3.09			9.71					
MAP-TP	7.75	14.22	2.94	5.88	2.04	2.00	2.53			8.34					
PL-T	11.64	23.14	6.08	2.30	0.59	11.07	1.30			2.43					
PL-TP	3.88	7.72	1.94	1.33	0.38	0.48	0.50			1.28					
MAP-T	19.91	30.16	11.75	31.27	16.26	39.17		17.92			20.37				
MAP-TP	9.67	14.57	3.25	10.72	4.99	2.04		6.53			9.17				
PL-T	12.93	25.48	6.67	2.48	0.59	22.35		5.01			4.96				
PL-TP	4.08	8.12	2.08	1.35	0.44	0.51		1.04			1.72				
MAP-T	21.13	37.08	10.00	20.29	8.84	37.92			7.28			6.88			
MAP-TP	11.76	17.67	2.90	11.76	3.99	2.04			4.69			5.38			
PL-T	11.68	23.28	6.05	2.36	0.55	10.87			1.26			2.62			
PL-TP	3.84	7.61	1.92	1.31	0.38	0.47			0.49			1.22			
MAP-T	85.97	181.33	57.16	37.04	19.75	99.16	38.87	56.63		110.31	139.88		104.23		
MAP-TP	10.35	16.23	3.32	11.29	5.84	2.31	5.01	9.90		23.82	27.37		12.72		
PL-T	16.18	32.14	8.28	3.57	0.67	26.48	4.06	12.67		12.95	24.55		11.99		
PL-TP	4.09	8.15	2.08	1.36	0.48	0.52	1.14	2.20		3.83	5.66		2.85		
MAP-T	80.71	156.66	50.69	71.25	37.62	95.05	55.99		82.99	163.15		192.55		133.43	
MAP-TP	17.30	23.16	3.71	15.53	6.12	2.40	7.53		8.50	33.21		28.37		16.38	
PL-T	18.46	35.40	9.64	2.85	1.00	17.46	9.46		10.23	31.85		32.80		21.54	
PL-TP	3.89	7.73	1.94	1.36	0.40	0.50	1.33		1.32	4.81		4.57		2.62	
MAP-T	43.02	68.44	29.96	64.64	30.11	76.02		65.23	33.52		58.50	35.49			69.90
MAP-TP	15.65	18.51	3.67	15.56	5.24	2.16		24.81	17.96		28.43	18.45			36.23
PL-T	15.66	30.79	8.02	2.92	0.89	22.98		10.29	3.27		9.07	4.38			12.36
PL-TP	4.65	9.29	2.37	1.45	0.55	0.61		4.02	1.53		4.31	2.67			4.95
MAP-T	175.90	325.45	75.37	123.68	90.06	105.02	113.92	568.67	350.10	435.09	1031.17	1288.62	597.04	742.05	532.18
MAP-TP	21.68	30.50	4.80	19.63	6.91	2.44	12.39	31.11	32.20	47.04	62.51	74.00	35.03	51.00	40.65
PL-T	50.93	100.73	27.42	6.49	2.95	44.39	47.06	34.96	24.48	120.99	66.05	98.96	49.97	76.30	72.79
PL-TP	4.75	9.42	2.42	1.46	0.61	0.65	1.45	4.63	2.86	5.52	9.30	6.91	4.16	3.76	5.36

TABLE II. Fisher matrix spectral decomposition—MAP, temperature only, adiabatic mode only. The eigenvalues and components of the unit eigenvectors are quoted in percent to keep the table compact. The eigenvectors are ordered such that the flattest direction appears in the last column. It is easily seen which combinations of cosmological parameters contribute to the different directions.

	Eigenvector					
	1	2	3	4	5	6
% error	0.18	0.41	1.30	3.05	21.65	46.49
$\delta h/h$	22.85	−68.66	−50.97	−3.78	−42.96	−17.50
$\delta\Omega_b/\Omega_b$	−14.46	−36.83	−32.64	12.66	68.17	50.61
$\delta\Omega_k$	−89.63	−11.17	−9.12	−35.73	−7.44	−20.66
$\delta\Omega_\Lambda/\Omega_\Lambda$	−35.06	−5.30	9.18	82.70	−37.00	21.20
$\delta n_s/n_s$	−2.41	61.35	−76.46	1.59	−14.23	13.42
τ_{reion}	0.72	−3.59	17.99	−41.31	−43.37	77.95

table, the same four sets of numbers are shown as one includes first one isocurvature mode and the corresponding adiabatic-isocurvature correlation, then two, and finally, all three isocurvature modes. (We remind the reader that the CDM isocurvature mode is observationally indistinguishable from the baryon isocurvature mode, so it is not included separately.) The table above demonstrates the breakdown of parameter estimation which occurs for the MAP temperature measurements when any two isocurvature modes are included. This breakdown is not directly attributable to any single isocurvature mode, and in fact the neutrino isocurvature velocity mode on its own has the least impact on parameter estimation. With the inclusion of all three isocurvature modes, the breakdown is catastrophic for the MAP temperature measurement alone. The situation improves once polarization is included, but the MAP experiment has not been optimized for a polarization measurement, and it is unlikely that the optimal level of noise (and zero foreground contamination) assumed here will actually be achieved. For Planck, only Ω_Λ and n_s are well determined with a temperature measurement alone, and even then many of the isocurvature amplitudes are only weakly constrained. With the inclusion of the polarization measurement, however, Planck is able to simultaneously set strong constraints on isocurvature amplitudes while accurately measuring the six cosmological parameters discussed here.

TABLE III. Fisher matrix spectral decomposition—MAP, temperature, and polarization, adiabatic mode only.

	Eigenvector					
	1	2	3	4	5	6
% error	0.18	0.40	1.25	1.91	3.38	16.41
$\delta h/h$	22.64	−68.81	−48.71	−15.74	0.59	−46.18
$\delta\Omega_b/\Omega_b$	−14.53	−36.83	−30.59	−8.73	22.03	83.28
$\delta\Omega_k$	−89.71	−11.05	−8.09	−12.86	−37.04	−15.07
$\delta\Omega_\Lambda/\Omega_\Lambda$	−34.96	−5.05	7.64	26.16	85.79	−25.48
$\delta n_s/n_s$	−2.32	61.19	−71.44	−29.12	15.87	−6.84
τ_{reion}	0.87	−4.11	38.27	−89.32	23.03	−3.07

TABLE IV. Fisher matrix spectral decomposition—MAP, temperature only, adiabatic mode, and three isocurvature modes.

	Eigenvector														
	1	2	3	4	5	6	7	8	9	10	11	12	13	14	15
% error	0.18	0.39	0.62	1.42	2.16	5.33	5.78	15.02	18.25	32.23	104.30	156.02	478.55	552.74	2041.56
$\delta h/h$	−22.37	−66.16	−23.66	−24.59	29.83	16.64	1.47	3.18	6.39	−11.01	21.28	−34.15	19.59	−24.78	0.35
$\delta\Omega_b/\Omega_b$	14.44	−34.94	−16.04	−8.80	21.57	−6.48	10.57	−36.81	−23.26	−21.55	−40.09	16.57	−50.21	28.34	−7.12
$\delta\Omega_k$	88.76	−9.49	−0.25	−8.48	11.45	15.41	−25.75	6.12	11.01	−8.41	19.85	12.18	7.71	−9.80	1.18
$\delta\Omega_\Lambda/\Omega_\Lambda$	34.67	−4.08	−6.77	36.94	−16.25	−8.86	42.60	−11.05	−15.21	14.05	−20.42	−63.60	13.50	−4.36	0.70
$\delta n_s/n_s$	2.25	59.67	−24.40	−50.00	36.57	19.02	2.09	−23.37	−1.20	1.18	−13.03	−29.43	6.18	−1.03	3.43
τ_{reion}	−0.69	−3.85	11.07	−3.59	−5.73	3.17	−23.11	36.66	57.46	−22.47	−55.86	−28.08	−11.74	8.69	−0.37
$\langle NIV,NIV\rangle$	−8.67	11.78	32.20	41.27	28.92	65.50	10.32	4.30	−9.90	−32.31	14.35	−8.84	−17.56	7.11	3.03
$\langle BI,BI\rangle$	−1.03	−13.84	49.58	−23.31	−19.71	26.50	−21.90	−29.97	−3.99	47.18	−8.15	−16.29	−23.27	−22.70	−26.57
$\langle NID,NID\rangle$	4.80	6.65	45.97	−23.13	18.52	−48.62	2.93	27.04	−31.81	−27.18	13.89	−23.47	−25.60	−21.64	14.82
$\langle NIV,AD\rangle$	−7.51	5.81	1.44	17.28	−13.55	−6.56	−43.68	−33.25	−26.65	−48.04	−24.71	−0.03	37.51	−32.15	−17.29
$\langle BI,AD\rangle$	3.51	−9.87	12.48	−21.80	−11.01	28.68	28.24	18.51	−23.52	5.23	−43.63	31.19	23.30	−26.77	49.58
$\langle NID,AD\rangle$	5.74	4.55	12.97	−23.73	−12.53	2.72	56.39	4.46	18.13	−29.62	1.67	18.81	11.71	−13.78	−62.93
$\langle NIV,BI\rangle$	1.75	−2.22	−17.69	−22.13	−31.27	22.99	−18.16	45.71	−52.50	−3.28	0.90	−15.91	3.26	38.60	−27.27
$\langle NIV,NID\rangle$	−0.34	3.25	−13.22	−19.69	−62.22	13.49	6.81	−25.08	15.00	−36.24	28.57	−13.83	−29.45	−4.08	35.62
$\langle BI,NID\rangle$	1.13	−13.35	44.69	−19.29	0.87	−7.25	3.57	−27.40	8.01	−9.72	6.35	−6.78	46.99	62.53	16.47

TABLE V. Fisher matrix spectral decomposition—MAP, temperature and polarization, adiabatic mode, and three isocurvature modes.

| | | | | | | | | Eigenvector | | | | | | | |
	1	2	3	4	5	6	7	8	9	10	11	12	13	14	15
% error	0.18	0.39	0.61	1.35	1.83	2.19	4.41	5.49	8.86	9.65	15.05	24.70	47.71	56.74	120.55
$\delta h/h$	−22.16	−66.25	−23.68	−21.54	24.45	21.56	−19.77	1.15	1.50	4.01	9.77	−42.55	−23.62	1.24	−12.53
$\delta\Omega_b/\Omega_b$	14.51	−34.90	−15.90	−7.99	12.55	16.76	8.09	14.65	36.53	−20.66	31.66	62.67	19.13	10.60	19.15
$\delta\Omega_k$	88.83	−9.31	−0.42	−6.58	9.23	9.47	−21.12	−24.16	−18.91	18.49	4.11	−6.60	0.56	−2.91	−2.41
$\delta\Omega_\Lambda/\Omega_\Lambda$	34.56	−3.81	−6.78	34.65	−17.58	−10.25	18.66	39.04	38.87	−41.22	−5.91	−35.64	−25.58	1.81	−9.23
$\delta n_s/n_s$	2.15	59.52	−23.48	−47.29	27.13	31.08	−16.67	2.66	17.10	−32.40	8.85	−13.21	−8.35	−3.57	−1.02
τ_{reion}	−0.83	−4.56	15.45	−12.76	−69.07	68.28	8.90	1.60	−6.66	0.93	2.58	−2.38	−1.74	−1.06	−0.06
$\langle NIV,NIV \rangle$	−8.70	11.79	31.96	44.31	13.19	24.80	−66.34	21.33	21.65	17.26	13.42	−3.31	7.52	8.83	8.03
$\langle BI,BI \rangle$	−0.95	−14.02	49.46	−21.29	−5.42	−16.45	−24.87	−25.26	−4.97	−51.00	−14.04	13.28	−20.31	41.86	−13.55
$\langle NID,NID \rangle$	4.92	6.41	45.97	−22.68	20.78	3.02	40.68	0.47	34.82	43.06	12.86	−12.54	−30.25	21.71	20.87
$\langle NIV,AD \rangle$	−7.56	5.88	1.33	17.35	−11.75	−7.70	−4.85	−45.77	21.65	−1.04	44.31	16.90	−42.71	−44.75	−27.27
$\langle BI,AD \rangle$	3.54	−10.01	12.49	−22.01	−4.01	−9.86	−21.96	30.57	−6.26	−0.69	−33.41	21.29	−38.89	−52.94	42.33
$\langle NID,AD \rangle$	5.75	4.37	12.89	−24.72	−3.17	−14.17	−3.70	58.20	−21.59	17.51	26.28	18.20	−6.26	−0.25	−61.03
$\langle NIV,BI \rangle$	1.69	−2.38	−17.07	−25.44	−27.17	−17.54	−23.68	−11.24	59.66	30.90	−41.80	5.86	16.40	3.18	−27.29
$\langle NIV,NID \rangle$	−0.43	3.13	−12.98	−23.05	−41.72	−42.83	−24.06	5.05	−1.57	3.36	50.76	−23.55	6.88	16.09	40.74
$\langle BI,NID \rangle$	1.23	−13.52	44.57	−17.98	8.09	−6.09	7.65	−2.22	14.70	−20.95	11.31	−27.64	57.21	−49.84	−6.00

TABLE VI. Fisher matrix spectral decomposition—Planck, temperature only, adiabatic mode only.

| | Eigenvector | | | | | |
	1	2	3	4	5	6
% error	0.03	0.20	0.27	1.59	5.07	27.52
$\delta h/h$	31.27	13.76	81.62	15.33	15.36	41.23
$\delta\Omega_b/\Omega_b$	−9.65	8.68	46.89	10.86	−26.91	−82.41
$\delta\Omega_k$	−87.67	13.33	25.96	−31.59	2.71	21.39
$\delta\Omega_\Lambda/\Omega_\Lambda$	−35.26	−25.01	−4.60	88.73	14.19	5.94
$\delta n_s/n_s$	−0.63	94.49	−21.05	24.43	5.62	−0.56
τ_{reion}	0.01	−2.03	1.29	−13.37	93.81	−31.87

With two isocurvature modes I_1 and I_2 there are five additional parameters: two autocorrelations $\langle I_1 I_1 \rangle$ and $\langle I_2 I_2 \rangle$, and three cross-correlations $\langle AI_1 \rangle$, $\langle AI_2 \rangle$, and $\langle I_1 I_2 \rangle$. Again there is a constraint on these parameters arising from the requirements of positive definiteness of the matrix-valued power spectrum. When all isocurvature modes are included, there are three isocurvature autocorrelations and six cross correlations. Given the large uncertainties (of order unity) in all cases except the Planck polarization and temperature measurement, the quadratic approximations employed are no longer accurate. Moreover, the large ratios between the largest and smallest eigenvalues make the calculations sensitive to small errors in computing the Fisher matrix elements, since the smallest eigenvalues control the largest errors. Nevertheless, the result that the errors in the parameters are large (of order unity) is reliable.

Tables II–V show the spectral decomposition (i.e., the eigenvectors and eigenvalues) of the Fisher matrix for the MAP satellite, and Tables VI–IX those for the Planck satellite, which illustrate the principal axes in likelihood space for the two experiments. The top row shows the 1-σ error, which is the inverse square root of the corresponding eigenvalue, expressed in percent. The other rows show the components of the normalized eigenvectors in each direction in parameter space, again in percent. The information shown provides a complete description of the likelihood function in the Gaussian approximation about the most probable, fiducial model. One easily reads off which combinations of cosmological parameters are best, and worst, determined.

TABLE VII. Fisher matrix spectral decomposition—Planck, temperature, and polarization, adiabatic mode only.

| | Eigenvector | | | | | |
	1	2	3	4	5	6
% error	0.02	0.17	0.21	0.45	1.13	8.68
$\delta h/h$	31.53	57.96	58.86	2.18	16.25	43.74
$\delta\Omega_b/\Omega_b$	−9.50	33.96	33.44	0.10	9.91	−86.83
$\delta\Omega_k$	−87.61	26.25	13.75	−2.95	−31.16	21.59
$\delta\Omega_\Lambda/\Omega_\Lambda$	−35.21	−23.49	10.46	9.17	89.09	8.88
$\delta n_s/n_s$	−0.49	65.09	−71.46	−2.30	25.51	0.90
τ_{reion}	0.04	−3.14	3.54	−99.48	8.91	1.03

TABLE VIII. Fisher matrix spectral decomposition—Planck, temperature only, adiabatic, and three isocuravture modes.

| | Eigenvector |
	1	2	3	4	5	6	7	8	9	10	11	12	13	14	15
% error	0.03	0.20	0.25	0.59	1.01	1.21	1.61	3.01	4.55	6.31	14.91	25.41	32.97	68.72	234.96
$\delta h/h$	−31.24	15.79	76.82	−14.11	−14.05	5.40	18.23	7.46	−7.39	13.29	−21.53	1.18	3.53	31.08	−19.62
$\delta\Omega_b/\Omega_b$	9.64	9.93	44.05	−5.39	−9.78	7.40	7.98	−1.22	−14.54	−5.79	41.38	−5.12	−13.46	−63.02	38.57
$\delta\Omega_k$	87.58	13.76	23.60	−9.13	−2.53	−8.72	−26.19	−7.75	−4.63	14.17	−9.95	0.34	3.70	14.85	−10.79
$\delta\Omega_\Lambda/\Omega_\Lambda$	35.22	−24.26	−3.13	14.12	−15.05	21.03	76.46	27.62	11.01	−21.69	−4.61	1.29	−1.50	8.14	−1.00
$\delta n_s/n_s$	0.63	91.37	−25.28	−14.07	−0.78	−1.48	25.33	3.66	6.10	−10.45	0.91	−0.07	2.36	1.42	1.08
τ_{reion}	−0.01	−2.17	1.15	−8.43	0.55	−14.13	−1.75	14.26	3.84	−9.64	−72.03	−33.87	30.22	−45.05	11.44
$\langle NIV,NIV\rangle$	−2.52	−9.68	−21.63	−31.82	−67.18	−11.48	14.49	−23.57	8.16	50.14	−3.23	−3.09	−2.50	1.45	19.97
$\langle BI,BI\rangle$	0.00	−10.18	4.28	−39.95	7.97	−54.69	5.15	16.78	23.99	−19.52	−8.05	42.93	−41.46	−13.66	−12.21
$\langle NID,NID\rangle$	2.35	−8.91	−15.98	−54.74	33.77	32.04	5.13	35.03	−44.37	28.79	−2.20	16.68	7.72	0.30	10.12
$\langle NIV,AD\rangle$	−1.89	0.93	−9.09	7.47	−29.01	−29.17	−7.64	51.75	−27.10	7.67	30.12	−29.12	8.77	−13.53	−51.19
$\langle BI,AD\rangle$	0.48	−5.25	7.82	−14.32	20.20	−2.28	13.29	−11.08	46.33	20.24	27.69	18.10	65.11	−21.05	−25.71
$\langle NID,AD\rangle$	2.15	−4.22	−3.27	−8.37	34.60	−3.30	32.88	−46.87	−13.09	21.39	−2.97	−39.23	−34.67	−18.15	−41.27
$\langle NIV,BI\rangle$	0.29	6.77	5.30	15.74	23.87	4.06	−6.45	42.75	51.71	48.65	2.53	−27.98	−30.75	5.22	20.47
$\langle NIV,NID\rangle$	0.42	2.37	2.67	36.43	24.30	−59.25	28.22	−2.26	−33.92	28.81	−0.27	15.30	19.52	11.33	32.13
$\langle BI,NID\rangle$	0.26	−12.07	4.47	−41.34	12.20	−25.54	3.23	−2.89	7.12	−32.70	27.31	−54.41	15.58	37.99	28.16

TABLE IX. Fisher matrix spectral decomposition—Planck, temperature and polarization, adiabatic, and three isocuravture modes.

| | Eigenvector |
	1	2	3	4	5	6	7	8	9	10	11	12	13	14	15
% error	0.02	0.17	0.20	0.28	0.39	0.45	0.76	1.06	1.25	1.38	2.51	5.23	7.81	10.77	12.66
$\delta h/h$	−31.47	55.52	55.35	−8.41	−21.63	4.14	7.58	12.62	11.02	−5.54	−3.07	15.41	−12.53	−29.10	−26.23
$\delta\Omega_b/\Omega_b$	9.49	32.46	31.06	−4.41	−13.33	1.11	3.15	10.34	5.48	−0.69	−6.86	−25.71	24.74	61.38	49.58
$\delta\Omega_k$	87.48	24.41	12.08	−6.80	−6.67	−2.47	7.43	−14.02	−23.18	13.66	−6.88	7.95	−5.75	−14.80	−13.07
$\delta\Omega_\Lambda/\Omega_\Lambda$	35.15	−21.92	8.36	12.82	−13.52	8.90	−9.56	40.19	66.56	−35.55	17.94	0.28	−2.49	−6.74	−3.72
$\delta n_s/n_s$	0.48	60.45	−68.10	−27.20	7.49	−3.08	3.87	4.73	20.77	−18.21	8.98	−3.25	1.07	−2.74	1.29
τ_{reion}	−0.04	−4.35	4.49	−14.17	−6.43	−94.42	−22.93	13.97	3.78	3.84	−6.24	−1.72	1.49	−2.43	−2.14
$\langle NIV,NIV\rangle$	−3.30	−23.79	−12.87	−36.34	−62.08	−0.39	46.28	23.57	−26.85	−7.84	18.41	−7.25	−13.96	4.00	0.16
$\langle BI,BI\rangle$	−0.01	−8.47	12.87	−25.18	6.01	−11.71	18.22	−55.69	26.19	−17.24	24.44	51.48	−18.35	30.28	6.19
$\langle NID,NID\rangle$	2.83	−14.59	9.28	−58.56	42.17	13.29	9.22	37.01	13.34	28.73	−32.18	13.28	−18.82	−3.98	16.40
$\langle NIV,AD\rangle$	−2.35	−5.76	−11.54	5.75	−23.11	−3.21	32.41	−9.23	33.06	36.21	−27.12	24.54	64.72	−12.57	−5.23
$\langle BI,AD\rangle$	0.70	0.10	13.40	−6.48	19.80	−5.05	8.52	4.03	−18.71	−16.94	42.56	10.46	33.51	−51.11	54.57
$\langle NID,AD\rangle$	2.52	−3.54	6.82	−6.65	31.63	−3.15	16.82	23.98	−29.86	−50.71	−10.46	18.24	41.56	25.21	−41.89
$\langle NIV,BI\rangle$	0.47	10.13	1.75	20.99	26.16	−9.68	26.61	27.78	3.31	49.38	60.86	1.35	−2.97	22.41	−23.00
$\langle NIV,NID\rangle$	0.43	4.11	−0.95	40.48	21.48	−22.75	65.82	−1.39	8.13	−19.26	−30.95	−15.06	−31.08	−10.03	18.48
$\langle BI,NID\rangle$	0.38	−9.88	17.82	−34.30	17.01	−1.32	15.47	−35.03	20.95	−3.18	12.84	−69.81	16.98	−12.29	−26.92
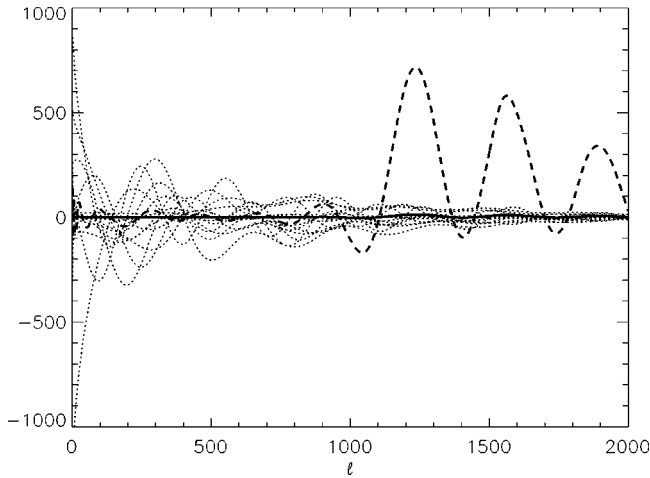
FIG. 2. Illustration of the degeneracy problem. Including isocurvature modes degrades the determination of the cosmological parameters by the MAP satellite temperature measurement. Above is shown how, for the most poorly measured eigenvector of the Fisher matrix, variations in the cosmological parameters and in the admixtures of the isocurvature modes and their correlations may be carefully chosen to cancel against each other. The individual contributions (plotted as the dotted curves) sum to the solid curve, which has been multiplied by 50 (indicated as the broken solid curve) for enhanced clarity.

It has frequently been emphasized that certain cosmological parameters, such as ω_b, ω_m, and the angular diameter distance d_A [given in Eq. (14)], are particularly well constrained by CMB anisotropy measurements. We found that the inclusion of isocurvature modes degrades the constraints on these special combinations as well, roughly in proportion to the degradation of the parameters they substitute. For example, the Planck temperature measurement with no isocurvature modes allowed yields an error of 1.18% and 0.89% for ω_m and ω_b, respectively, whereas with the inclusion of three isocurvature modes these errors degrade to 6.30% and 3.54%, respectively. This is because the covariances between these parameters and the isocurvature correlation amplitudes are non-negligible.

IV. DISCUSSION

We have considered to what extent it will be possible to test the hypothesis that the primordial perturbations were adiabatic. In our view, since the theoretical situation is ambiguous, such a check is essential in order for us to reliably interpret the CMB anisotropy as a reliable probe of cosmological parameters. We find that the MAP satellite alone, even with an optimistic assumption about the polarization measurement, will be unable to set useful limits on the amplitudes of isocurvature modes. The Planck satellite promises to be much more powerful in this respect and will be able to limit the amplitudes of isocurvature modes to less than 10% of the adiabatic mode.

We explore how much the errors in determining cosmological parameters from the CMB alone degrade as an increasing number of isocurvature modes is admitted. When in addition to the adiabatic mode only one isocurvature mode is

allowed, MAP (with polarization) can still place quite stringent constraints on the possible contribution of the isocurvature modes, and the increase in the errors in determining the other cosmological parameters is quite modest. However, when more than one isocurvature mode and the corresponding correlations are considered, the errors increase quite dramatically. Moreover, in this case, only very weak limits on the contamination of the adiabatic mode with isocurvature modes are possible. In the case of all three isocurvature modes, the fractional errors become of order one, even when polarization information is taken into account. The degeneracy introduced by the inclusion of nonadiabatic modes is illustrated in Fig. 2. Without a polarization measurement, admitting isocurvature modes ruins MAP's ability to measure cosmological parameters. The behavior observed is likely simply the result of the model possessing too many degrees of freedom. For all models considered, the CMB moments are rather smooth, slowly varying functions of l, so that a spline passing through a rather modest number of points would quite accurately characterize any of the theoretical models. Hence, in practice for parameter estimation the CMB data contains much less useful information than one might naively conclude if one argued that all of the C_l's are independent. Rather than $l_{max} \approx 1000$, the true number of independently measured numbers is closer to 10.

The situation is improved if we consider the Planck's estimated sensitivities. Planck has been designed to measure polarization accurately and so the estimated errors here may be more realistic than those for MAP. Our results demonstrate that there is a high payoff for an accurate measurement of the polarization. Table I shows that even when we allow all possible isocurvature modes with arbitrary cross correlations, Planck can set upper limits of less than 10% on the isocurvature mode auto- and cross-correlation power relative to the adiabatic power. Simultaneously, Planck can constrain the most interesting cosmological parameters to a few percent or better.

In conclusion, this study has focused on one difficulty in interpreting the CMB anisotropy data, namely in checking the assumption that the primordial perturbations were adiabatic. We have made severe idealizations in other respects, namely assuming Gaussianity and uniform noise, and in ignoring foreground contamination. Dealing with these issues will pose massive challenges for the real experiments. Nevertheless, the calculations reported here do offer a clear goal and a lesson, namely that high precision measurements of the polarization, in addition to the temperature of the cosmic microwave sky, will likely be essential to a conclusive understanding of the nature of the primordial perturbations.

[1] C. Bennet *et al.*, Astrophys. J. Lett. **464**, L1 (1996).

[2] A. Miller *et al.*, Astrophys. J. Lett. **524**, L1 (1999).

[3] P. de Bernardis *et al.*, Nature (London) **404**, 955 (2000).

[4] S. Hanany *et al.*, Astrophys. J. Lett. **545**, L5 (2000).

[5] http://map.gsfc.nasa.gov/

[6] http://astro.estec.esa.nl/SA-general/Projects/Planck/

[7] See, for example, J.R. Bond, G. Efstathiou, and M. Tegmark, Mon. Not. R. Astron. Soc. **291,** L33 (1997); L. Knox, Phys. Rev. D **52**, 4307 (1995); G. Jungman, M. Kamionkowski, A. Kosowsky, and D. Spergel, Phys. Rev. Lett. **76**, 1007 (1996); M. Zaldarriaga, D.N. Spergel, and U. Seljak, Astrophys. J. **488**, 1 (1997). A recent reference is W. Hu, M. Fukugita, M. Zaldarriaga, and M. Tegmark, *ibid.* **549**, 669 (2001).

[8] S.W. Hawking, Phys. Lett. **115B**, 295 (1982); A.A. Starobinsky, *ibid.* **117B**, 125 (1982); A. Guth and S.Y. Pi, Phys. Rev. Lett. **49**, 1110 (1982); J. Bardeen, P. Steinhardt, and M. Turner, Phys. Rev. D **28**, 679 (1983).

[9] A. Liddle and D. Lyth, *Cosmological Inflation and Large-Scale Structure* (Cambridge University Press, Cambridge, England, 2000).

[10] See, for example, D.S. Salopek, Phys. Rev. D **45**, 1139 (1992); L. Kofman and A. Linde, Nucl. Phys. **B282**, 555 (1987); E. Vishniac, K. Olive, and D. Seckel, *ibid.* **B289**, 717 (1987); L. Kofman A. Linde, and J. Einasto, Nature (London) **326**, 48 (1987); H. Hodges and J. Primack, Phys. Rev. D **43**, 3155 (1991); A. Linde, Phys. Lett. B **284**, 215 (1992); R. Basu, A. Guth, and A. Vilenkin, Phys. Rev. D **44**, 340 (1991); L. Kofman, Phys. Lett. **173B**, 400 (1986); M. Bucher and Y. Zhu, Phys. Rev. D **55**, 7415 (1997), and references therein.

[11] M. Bucher, K. Moodley, and N. Turok, Phys. Rev. D **62**, 083508 (2000).

[12] P.J.E. Peebles, Nature (London) **327**, 210 (1987); Astrophys. J., Lett. Ed. **315**, L73 (1987); Astrophys. J. **510**, 523 (1999); **510**, 531 (1999).

[13] J.R. Bond and G. Efstathiou, Mon. Not. R. Astron. Soc. **22**, 33 (1987).

[14] R. Cen, J.P. Ostriker, and P.J.E. Peebles, Astrophys. J. **415**, 423 (1993).

[15] J.R. Bond and G. Efstathiou, Mon. Not. R. Astron. Soc. **218**, 103 (1986).

[16] A. Rebhan and D. Schwarz, Phys. Rev. D **50**, 2541 (1994).

[17] A. Challinor and A. Lasenby, Astrophys. J. **513**, 1 (1999).

[18] R. Stompor, A.J. Banday, and K.M. Gorski, Astrophys. J. **463**, 8 (1996).

[19] N. Gouda and N. Sugiyama, Astrophys. J. Lett. **395**, L59 (1992).

[20] K. Gorski and J. Silk, Astrophys. J. Lett. **346**, L1 (1989).

[21] J. Yokoyama and Y. Suto, Astrophys. J. **379**, 427 (1991).

[22] T. Suginohara and Y. Suto, Astrophys. J. **387**, 431 (1992).

[23] T. Chiba, N. Sugiyama, and Y. Suto, Astrophys. J. **429**, 427 (1994).

[24] W. Hu, E. Bunn, and N. Sugiyama, Astrophys. J. Lett. **447**, L59 (1995).

[25] N. Sugiyama, M. Sasaki, and K. Tomita, Astrophys. J. Lett. **338**, L45 (1989).

[26] J. Yokoyama, Astropart. Phys. **2**, 291 (1994).

[27] K. Enqvist and H. Kurki-Suonio, Phys. Rev. D **61**, 043002 (2000); K. Enqvist, J. Valiviita, and H. Kurki-Suonio, *ibid.* **62**, 103003 (2000).

[28] E. Pierpaoli, J. García-Bellido, and S. Borgani, J. High Energy Phys. **10**, 15 (1999).

[29] A. Linde and S. Mukhanov, Phys. Rev. D **56**, 535 (1997).

[30] D. Langlois, Phys. Rev. D **59**, 123512 (1999).

[31] D. Langlois and A. Riazuelo, Phys. Rev. D **62**, 043504 (2000).

[32] D. Polarski and A.A. Starobinskii, Phys. Rev. D **50**, 6123 (1994).

[33] Y. Wang, D. Spergel, and M. Strauss, Astrophys. J. **498**, 1 (1998).

[34] U. Seljak and M. Zaldarriaga, Astrophys. J. **469**, 437 (1996).

[35] D.J. Eisenstein, W. Hu, and M. Tegmark Astrophys. J. **518**, 2 (1999).